Processing and Application of Ceramics 14 [1] (2020) 71–76
https://doi.org/10.2298/PAC2001071S

Luminescence properties of Eu^{3+} activated Y_2MoO_6 powders calcined at different temperatures

Nadežda Stanković[1,*], Marko Nikolić[2], Branislav Jelenković[2], Nina Daneu[3], Jelena Maletaškić[4], Marija Prekajski Đorđević[4], Branko Matović[4]

[1]*Vinča Institute of Nuclear Science, Department of Atomics Physics, PO Box 522, 11000 Belgrade, Serbia*
[2]*Institute of Physics Belgrade, University of Belgrade, Pregrevica 118, 11000 Belgrade, Serbia*
[3]*Jožef Stefan Institute, Advanced Materials Department, Jamova 39, 1000 Ljubljana, Slovenia*
[4]*Vinča Institute of Nuclear Science, Material Science Laboratory, PO Box 522, 11000 Belgrade, Serbia*

Received 15 August 2019; Received in revised form 9 January 2020; Accepted 2 March 2020

Abstract

In the last decade, an immense progress has been made in white LEDs, mainly due to the development of red-emitting phosphors. In this paper, we report on the synthesis of Eu^{3+} activated Y_2MoO_6 by a self-initiated and self-sustained method. The obtained powder was calcined at various temperatures in the 600–1400 °C range and examined by X-ray diffraction (XRD), scanning electron microscopy (SEM), transmission electron microscopy (TEM) and photoluminescence spectroscopy (PL). The results revealed that all powders are single phase Y_2MoO_6:Eu^{3+}, with particle size in the nanorange at lower treatment temperatures (600 and 800 °C) and in the microrange at higher calcination temperatures (1000–1400 °C). The obtained powders are promising materials for white light-emitting diodes as they can efficiently absorb energy in 324–425 nm region (near-UV to blue light region) and emit at 611 nm in the red region of the spectrum, while exhibiting high thermal and chemical stability.

Keywords: *powders, doping, luminescence, transmission electron microscopy (TEM), optical devices*

I. Introduction

Light-emitting diodes (LEDs) are solid-state lighting sources used in display backlighting (mobile phones, cameras, notebooks, monitors, electric scoreboards, outdoor billboards, signage lighting, etc.), medical services, general illumination and communications [1–7]. In the last few years, there is a tendency for LEDs to generate white light. For generating white light, blue LED chips with red/green/blue/orange/yellow phosphors have been investigated [7]. This led to the considerable research of new phosphor materials, the key one being red-emitting phosphors. This is due to the fact that red-emitting phosphors can help transform cold blue light to warm white light. Red phosphors consist of an activator doped with various rare earth elements at specific positions in the host lattice. As red phosphors, various compounds doped with Eu^{2+}, Ce^{3+}, Eu^{3+}, Sm^{3+} have been investigated and in the case of Eu^{2+} and Ce^{3+}, the phosphors show a broad peak in the orange-reddish region [8–10]. On the other hand, doping with Eu^{3+} exhibits narrow emission bands in the 590–630 nm range with the central emission band at around 611 nm when $Eu_3{}^+$ resides in a non-centrosymmetric site of the host material; a sharp excitation peak is also present at ~400 nm. These characteristics of the emission spectra are due to the intraconfigurational $4f$–$4f$ transitions [11]. One of the materials in which Eu^{3+} occupies the non-centrosymmetric sites is Y_2MoO_6 that exhibits excellent thermal and chemical stability [12–14]. In literature, various synthesis methods for Y_2MoO_6 have been reported including sol-gel [15–18], molten salt [13] and solid-state [14,18,19]. Herein, we report an investigation of 5 at.% Eu^{3+} doped Y_2MoO_6 powders, prepared by a novel self-propagating method, which is simple and inexpensive and, to the best of our knowledge, it has not yet been utilized for Y_2MoO_6 synthesis. In order to explore the thermal stability of these powders, they have been calcined at various temperatures to obtain single-

* Corresponding author: tel: +381 11 3408 782,
e-mail: *nadezdas@vinca.rs*

phase products. Since the influence of different concentrations of Eu^{3+} has been previously reported [13,14], the focus of the study presented in this manuscript was on the stability of the Y_2MoO_6 phase in a wide range of temperatures.

II. Experimental details

The Y_2MoO_6 was doped with 5 at.% of Eu_3^+ as the activator by mixing yttrium(III) nitrate hexahydrate $Y(NO_3)_3 \cdot 6\,H_2O$ (99.9%), ammonium molybdate tetrahydrate $(NH_4)_6Mo_7O_{24} \cdot 4\,H_2O$ (99%), europium(III) nitrate $Eu(NO_3)_3$ (99.9%) and sodium hydroxide NaOH (>98.5%) in an agate mortar, in air at room temperature. A self-initiated and self-sustained reaction started with NH_4OH and water vapour release immediately during the grinding of the mixture followed by the release of heat. The solid-state reaction is presented with the following equation:

$$13.3Y(NO_3)_3 \cdot 6\,H_2O + (NH_4)_6Mo_7O_{24} \cdot 4\,H_2O + 42\,NaOH + 0.7Eu(NO_3)_3 \longrightarrow 7\,Y_{1.90}Eu_{0.1}MoO_6 + 42\,NaNO_3 + 6\,NH_4OH + xH_2O \quad (1)$$

The product was purified by washing in order to remove $NaNO_3$, NH_4OH and the unreacted NaOH. The mixture was then re-suspended in distilled water and centrifuged 3 times for 15 min (~4000 rpm) followed by another centrifugation step in ethanol for 15 min (~4000 rpm). The product was subsequently dried in air at 80 °C to yield ultrafine powder (~1 g) that was further annealed in air for 4 h at various temperatures (600–1400 °C).

The phase composition of the calcined Eu^{3+} activated Y_2MoO_6 powders was determined using X-ray diffraction (Rigaku Ultima IV, Japan). The X-ray beam was nickel-filtered CuKα_1 radiation (λ = 0.1540 nm, operating at 40 kV and 40 mA). The XRD data were collected from 20 to 70° (2θ) with the 0.02° step size at a scanning rate of 5 °/min. The morphology and particle size were examined by scanning electron microscopy (JSM-7600F, JEOL, Japan). Transmission electron microscopy (TEM) analyses were performed on a 200 kV microscope (JEM-2100, JEOL, Japan) with LaB_6 electron source equipped with an EDS spectrometer. The Ocean Optics spectrometer (HR2000) was used to measure the luminescence emission spectra of the Y_2MoO_6 : 5 at.% Eu^{3+} samples. The excitation source was a focused diode laser with a 405 nm line. The luminescence excitation spectra were measured with Spex Fluorolog spectrofluorometer with 500 W Xenon lamp as the excitation source.

III. Results and discussion

Figure 1 presents XRD diagrams of the samples calcined at temperatures between 600 and 1400 °C for 4 h, which shows that all samples are single phase pure monoclinic Y_2MoO_6 (JCPDS card 00-057-0517). The diagram for 600 °C shows only broad and weak peaks of the major reflections suggesting that the powder is nanosized or poorly crystalline. With the increase of temperature, at 800 °C, sharper reflections appear indicating the beginning of crystallization or grain growth, while the sharpest reflections are observed in the samples heated at 1000 and 1200 °C. Although the reported melting temperature of Y_2MoO_6 is 1310 °C [20], sample heated for 4 h at 1400 °C shows only a slight decrease in intensity, suggesting that melting temperature is higher than the reported and that at 1400 °C melting only starts to occur.

From the XRD patterns we calculated unit cell parameters (a, b, c) of the samples calcined at different temperatures and results are presented in Table 1. The structure of Y_2MoO_6 comprises of zigzag MoO_5 polyhedral rows distributed through the YO_8 framework along the c-direction [001]. Molybdenum is coordinated with five oxygen atoms into strongly distorted bipyramidal units [19]. The expansion of the unit cell in the

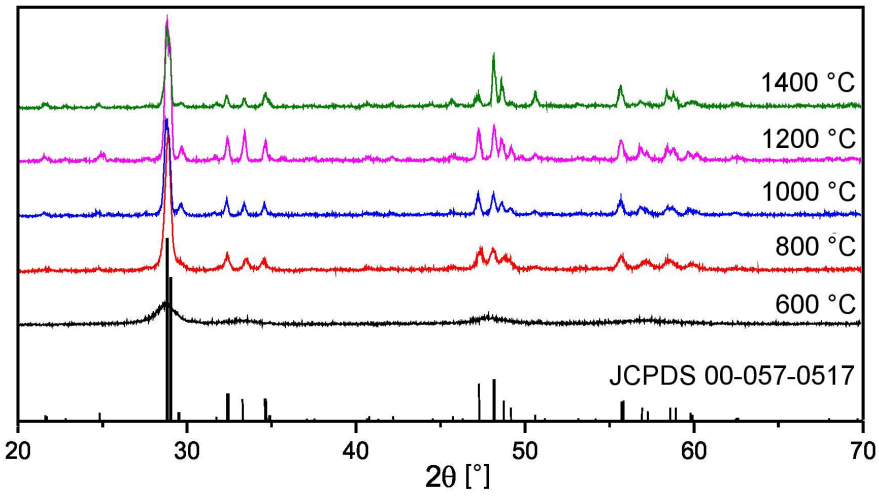

Figure 1. XRD diagrams of Y_2MoO_6 : 5 at.% Eu^{3+} samples calcined at different temperatures (JCPDS card 00-057-0517 is also presented at the bottom as the reference for obtained diagrams)

Table 1. Lattice parameters (a, b, c) of Y_2MoO_6 : 5 at.% Eu^{3+} annealed at various temperatures

Temperature [°C]	a [Å]	b [Å]	c [Å]
600	16.970(6)	10.925(12)	5.334(19)
800	16.430(4)	11.056(2)	5.343(11)
1000	16.386(2)	11.049(16)	5.357(8)
1200	16.374(2)	11.041(11)	5.359(6)
1400	16.371(3)	11.042(18)	5.359(10)

c-direction and its shrinkage in the a-direction suggest deformation of these polyhedra and change in the length of the Y–O bond. The length of Y–O is changing due to Eu^{3+} substitution of the Y^{3+} in the structure [11]. This substitution is possible since the Y^{3+} (1.019 Å, CN = 8) and Eu^{3+} (1.066 Å, CN = 8) have similar ionic radii [13,21]. On the other hand, Mo–O bonds do not change significantly, suggesting that Y atoms are overbonded and Mo atoms are underbonded, i.e. Y–O bonds are under compressive stress (shrinkage) and Mo–O are under tensile stress (expansion) [19].

SEM micrographs of the samples calcined at different temperatures (Fig. 2) clearly show an increase of Y_2MoO_6 grain size with temperature. At 600 and 800 °C the grains are in the nanorange and highly agglomerated. Densification accompanied by grain growth (coarsening) can be observed in the initial stage of sintering, i.e. after calcination at 800 °C. At 1000 °C (Fig. 2c), the nanosized grains grow up to ~500 nm, the sample shows uniform grain size distribution and occasional formation of crystals with well-developed crystal faces due to the growth under unconstrained conditions. Evidence for the grain growth by solid-state diffusion and the formation of necks between the neighbouring Y_2MoO_6 grains is observed in Fig. 2c. At 1200 °C (Fig. 2d), the coarsening process continues, leading to the formation of even larger grains ranging from 0.5 μm to several microns. After calcination at 1400 °C, the well-developed crystal faces are no longer observed (Fig. 2e), indicating the beginning of the melting process, also observed by XRD analyses.

The samples heated at 600 and 800 °C, with grain size in the nanorange, were additionally analysed by transmission electron microscopy (TEM). Low-magnification images of both samples with insets of the selected area electron diffraction (SAED) patterns and energy dispersive spectrum (EDS) are shown in Fig. 3. The sample heated at 600 °C has particle size in the range of ~10 nm (see enlarged image of an individual grain in the top left inset of Fig. 3a) which results in SAED with full diffraction rings with d-spacings corresponding to the Y_2MoO_6 phase (JCPDS card 00-057-0517). The sample calcined at 800 °C has larger average grain size of ~30–50 nm (see the top left inset in Fig. 3b) and hence gives spotted diffraction rings with d-values corresponding to the Y_2MoO_6 phase. EDS analyses of

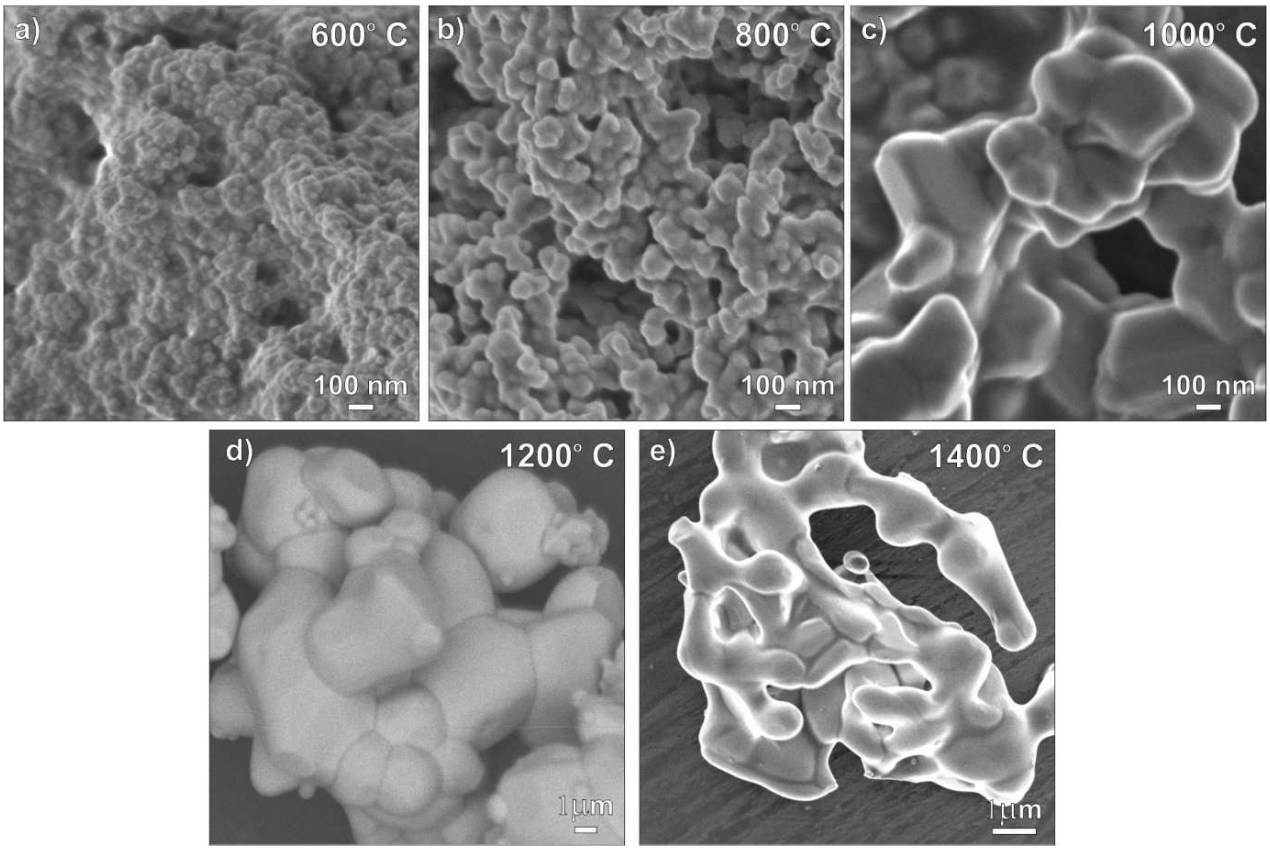

Figure 2. SEM micrographs of Y_2MoO_6 : 5 at.% Eu^{3+} at various temperatures; a) 600 °C, b) 800 °C, c) 1000 °C, d) 1200 °C and e) 1400 °C

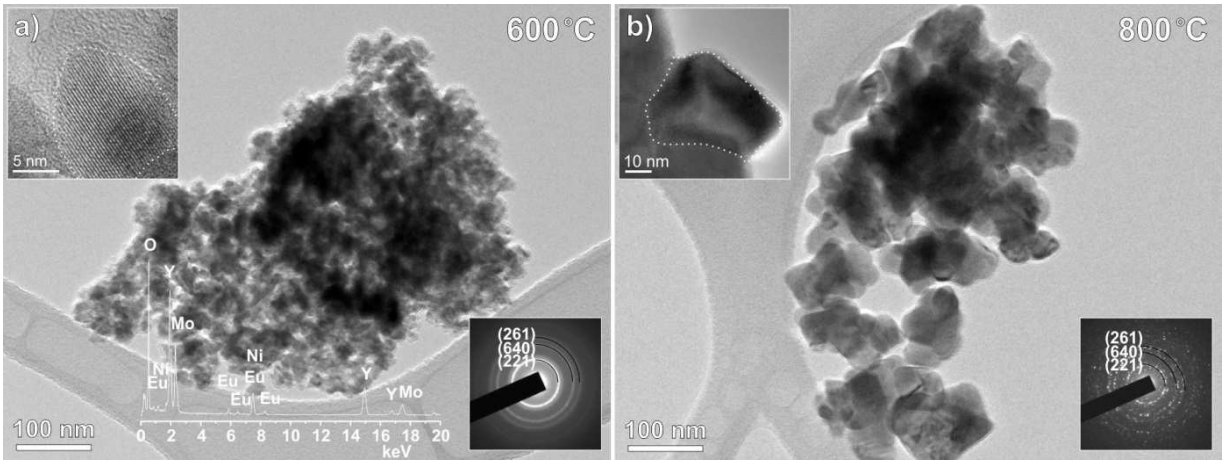

Figure 3. TEM micrographs of Y_2MoO_6 : 5 at.% Eu^{3+} with corresponding selected area diffraction (SAED) patterns in the bottom right corner and single grains in the top left corner, at a) 600 °C and b) 800 °C

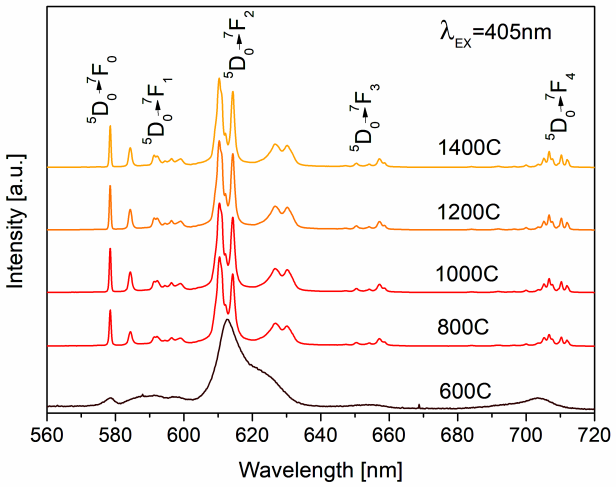

Figure 4. Emission spectra of samples calcined at various temperatures with λ_{ex} = 405 nm

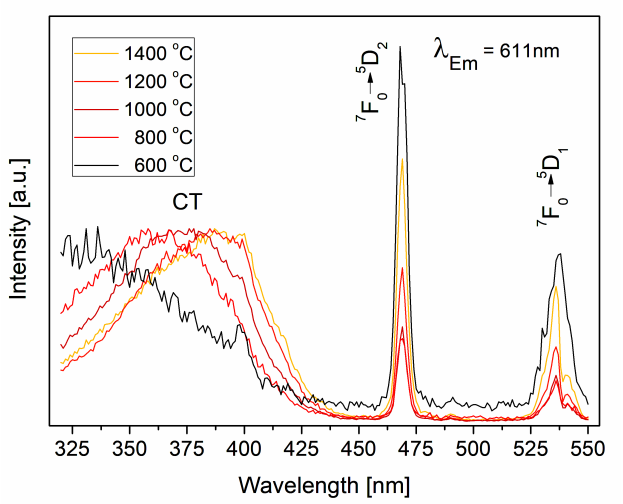

Figure 5. Excitation spectra of samples calcined at various temperatures with λ_{em} = 611 nm broad emission band in emission spectra

both samples were performed to confirm the incorporation of Eu into the Y_2MoO_6 phase. Single EDS spectra were taken on the whole clusters, individual grains, as well as on grain boundaries. The analyses have shown that Eu is uniformly distributed in both samples, it is not segregated at the grain boundaries and does not form any secondary phase as found by XRD analyses.

Photoluminescence emission spectra of the Y_2MoO_6 : 5 at.% Eu^{3+} samples calcined at various temperatures are presented in Fig. 4. Fixed concentration of 5 at.% Eu^{3+} was used in order to keep the influence of concentration quenching effect to a minimum. It can be noted that the Y_2MoO_6 : 5 at.% Eu_3^+ powder annealed at 600 °C has a broad emission band as a result of the small grain size and disordered structure, i.e. the difference in the bond length and the presence of distorted MoO_5 and YO_8:Eu_3^+ polyhedra. The increase of temperature leads to the ordering of MoO_5 and YO_8:Eu_3^+ units, previously shown as the change of unit cell parameters in XRD (Table 1) inducing to an increase in luminescence intensity and the appearance of narrow emission lines. Narrow lines, high in intensity, both in emission and excitation spectra (Figs. 4 and 5) are the result of $4f$–$4f$ transition in Eu^{3+} ions [11]. The photoluminescence spectra show that the samples exhibit the characteristic emission peak of Eu_3^+ ions at 611 nm (orange-reddish part of the spectrum) and that the emission is not changing with the increase of calcination temperature. Even though the phosphor calcined at 1400 °C exhibited initial melting, it still shows high brightness.

As already mentioned, incorporation of Eu^{3+} into non-symmetric crystallographic positions is very important for the luminescence properties. The Eu^{3+}-activated phosphors emit in the orange part of the visible spectrum if the Eu^{3+} ion occupies a site with a centre of symmetry in the host lattice and in the red or infrared if it occupies a site which is not a centre of symmetry [22]. In the excitation spectrum (Fig. 5), broad absorption lines at 324 nm to 425 nm are the result of electron charge transfer (CT) from MoO_6^{2+} to Eu^{3+} and with the increase in temperature, the CT region shrinks and shifts to lower energies [11]. The photoluminescence properties of the samples heated at ≥800 °C are

not changed and all of the samples show that Y_2MoO_6 : 5 at.% Eu^{3+} can efficiently absorb energy in the near-UV region and as a result emit in the red region of the spectrum. It can be only seen that the intensity of emission lines increases with the increase in temperature, due to the higher crystallinity. A high degree of crystallinity and predominantly spherical grain morphology of these samples generate high brightness and resolution of PL spectra.

IV. Conclusions

The Y_2MoO_6 : 5 at.% Eu^{3+} phosphor was successfully synthesized by a simple and low-cost self-propagating method and calcined in the temperature range from 600 to 1400 °C. The single phase samples were obtained at all temperatures with an increase in grain size from ~5 nm (600 °C), to a few microns (1200 °C). The obtained powders efficiently absorb energy in the near-UV and blue region (324–425 nm) and emit in the red region of the spectrum (611 nm) which makes them a promising material for red phosphors in white light-emitting diodes. This investigation shows that the optimal temperature for calcination of the Y_2MoO_6 : 5 at.% Eu^{3+} phosphor is 800 °C, since the emission is not changing with the increase of calcination temperature.

Acknowledgments: This work was supported by the Ministry of Education, Science and Technological Development of the Republic of Serbia, under contract No. III45012. This work has been enabled through the Slovenian-Serbian bilateral collaboration under the project No. 06-00-118/2018-09/51: Synthesis of luminescent nanopowders of type R_2MoO_6:REE and their structural characterization by means of electron microscopy. Financial support from the Slovenian Research Agency (research core funding No. P2-0091) is also gratefully acknowledged.

References

1. M.R. Krames, O.B. Shchekin, R. Mueller-Mach, G.O. Mueller, L. Zhou, G. Harbers, M.G. Craford, "Status and future of high-power light-emitting diodes for solid-state lighting", *J. Disp. Technol.*, **3** (2007) 160–175.
2. D.A. Steigerwald, J.C. Bhat, D. Collins, R.M. Fletcher, M.O. Holcomb, M.J. Ludowise, P.S. Martin, S.L. Rudaz, "Illumination with solid state lighting technology", *IEEE J. Selected Topics Quantum Electron.*, **8** (2002) 310–320.
3. F.M. Steranka, J. Bhat, D. Collins, L. Cook, M.G. Craford, R. Fletcher, N. Gardner, P. Grillot, W. Goetz, M. Keuper, R. Khare, A. Kim, M. Krames, G. Harbers, M. Ludowise, P.S. Martin, M. Misra, G. Mueller, R. Mueller-Mach, S. Rudaz, Y.C. Shen, D. Steigerwald, S. Stockman, S. Subramanya, T. Trottier, J.J. Wierer, "High power LEDs – Technology status and market applications", *Phys. Status Solidi A*, **194** (2002) 380–388.
4. E.F. Schubert, K. Jong Kyu, L. Hong, J.Q. Xi, "Solid-state lighting - A benevolent technology", *Rep. Prog. Phys.*, **69** (2006) 3069.
5. Y. Aoyama, T. Yachi, "An LED module array system designed for streetlight use", pp. 1–5 in *2008 IEEE Energy 2030 Conference*, Atlanta, GA, 2008.
6. R. Vittori, A. Scaburri, "New solid state technologies and light emission diodes as a mean of control and lighting source applicable to explosion proof equipment, with the scope to reduce maintenance, to limit the risk of bad maintenance and to expand the plants' life", pp. 193–198 in *2009 Conference Record PCIC Europe*, Barcelona, 2009.
7. M.-H. Chang, D. Das, P.V. Varde, M. Pecht, "Light emitting diodes reliability review", *Microelectron. Reliab.*, **52** (2012) 762–782.
8. X.-H. He, Y. Zhu, "Improvement of morphology and luminescence of CaS:Eu^{2+} red-emitting phosphor particles via carbon-containing additive strategy", *J. Mater. Sci.*, **43** (2008) 1515–1519.
9. X.H. He, N. Lian, J.H. Sun, M.Y. Guan, "Dependence of luminescence properties on composition of rare-earth activated (oxy)nitrides phosphors for white-LEDs applications", *J. Mater. Sci.*, **44** (2009) 4763–4775.
10. V. Bachmann, C. Ronda, A. Meijerink, "Temperature quenching of yellow Ce^{3+} luminescence in YAG:Ce", *Chem. Mater.*, **21** (2009) 2077–2084.
11. K. Deng, T. Gong, Y. Chen, C. Duan, M. Yin, "Efficient red-emitting phosphor for near-ultraviolet-based solid-state lighting", *Opt. Lett.*, **36** (2011) 4470–4472.
12. Y. Chen, J. Wang, C. Liu, X. Kuang, Q. Su, "A host sensitized reddish-orange Gd_2MoO_6:Sm_3^+ phosphor for light emitting diodes", *Appl. Phys. Lett.*, **98** (2011) 081917.
13. X. He, D. Bian, H. Wang, J. Xu, "Eu^{3+}-activated Y_2MoO_6: A narrow band red-emitting phosphor with strong near-UV absorption", *Luminescence*, **28** (2013) 973–976.
14. B. Han, J. Zhang, Z. Wang, Y. Liu, H. Shi, "Investigation on the concentration quenching and energy transfer of red-light-emitting phosphor Y_2MoO_6:Eu^{3+}", *J. Lumin.*, **149** (2014) 150–154.
15. L. Wu, X. Tian, K. Deng, G. Liu, M. Yin, "Site selective spectroscopic study of an efficient red-emitting phosphor Y_2MoO_6:Eu", *Opt. Mater.*, **45** (2015) 28–31.
16. H. Li, S. Zhang, S. Zhou, X. Cao, Y. Zheng, "Crystalline size effect on the energy transfer from Mo-O groups to Eu^{3+} ions in R_2MoO_6:Eu (R = La, Gd, and Y) crystals", *J. Phys. Chem. C*, **113** (2009) 13115–13120.
17. M. Pang, X. Liu, J. Lin, "Luminescence properties of R_2MoO_6:Eu^{3+} (R = Gd, Y, La) phosphors prepared by Pechini sol-gel process", *J. Mater. Res.*, **20** (2005) 2676–2681.
18. M. Wang, H. Zhang, L. Li, X. Liu, F. Hong, R. Li, H. Song, M. Gui, J. Shen, W. Zhu, J. Wang, L. Zhou, J.H. Jeong, "Charge transfer bands of Mo–O and photoluminescence properties of micro-material Y_2MoO_6:Eu^{3+} red phosphor", *J. Alloy. Compd.*, **585** (2014) 138–145.
19. J.A. Alonso, F. Rivillas, M.J. Martínez-Lope, V. Pomjakushin, "Preparation and structural study from neutron diffraction data of R_2MoO_6 (R = Dy, Ho, Er, Tm, Yb, Y)", *J. Solid State Chem.*, **177** (2004) 2470–2476.
20. J. Fournier, J. Fournier, R. Kohlmuller, "Etude des systemes La_2O_3-MoO_3, Y_2O_3-MoO_3, et des phases Ln_6MoO_{12}", *Bull. Soc. Chim. Fran.*, **12** (1970) 4277–4283.
21. R.D. Shannon, "Revised effective ionic radii and systematic studies of interatomic distances in halides and chalcogenides", *Acta Crystallogr. A*, **32** (1976) 751–767.

22. G. Blasse, "Chemistry and physics of R-activated phosphors", pp. 237–274, , Ch. 34 in *Handbook on the Physics and Chemistry of Rare Earths*. Eds. K.A. Gschneidner, Jr., L. Eyring, Elsevier, 1979.